

# The Münster cluster-jet target for the future $\bar{P}$ ANDA experiment

Sophia Vestrick<sup>1\*</sup>, Philipp Brand<sup>1</sup>, Daniel Bonaventura<sup>1</sup>, Hanna Eick<sup>1</sup>, Christian Mannweiler<sup>1</sup>, and Alfons Khoukaz<sup>1</sup>

<sup>1</sup>Westfälische Wilhelms-Universität Münster, Institut für Kernphysik, Wilhelm-Klemm-Straße 9, 48149 Münster, Germany

**Abstract.** For high precision storage ring experiments as the future  $\bar{P}$ ANDA experiment, very sophisticated internal targets have to be used. For this purpose, a state-of-the-art cluster-jet target was developed at the University Münster. Basically, hydrogen is cooled to cryogenic temperatures and pressed through a specially shaped Laval nozzle to form a cluster-jet expanding into vacuum. Due to the stability and large mass of the clusters, a practically undisturbed flight path in vacuum of above 5 m is possible, leading to manifold possible applications, including the interaction with a storage ring beam at a distance of 2.25 m as desired for the  $\bar{P}$ ANDA experiment. With a first prototype target, the “proof-of-principle” was delivered, and after first improvements the world record in target thickness in such large distance to the nozzle was measured. Based on this work, the final  $\bar{P}$ ANDA cluster-jet target was developed and built up, and is presented in this article.

## 1 Introduction

The  $\bar{P}$ ANDA experiment (antiProton ANihilation at Darmstadt) will investigate antiproton proton collisions with the utmost precision at the antiproton high energy storage ring (HESR) at the facility for antiproton and ion research (FAIR), which is currently under construction. It aims to address fundamental questions of the quantum chromodynamics, i.e., the theory of strong interaction and hadron physics [1,2]. The antiprotons with a beam momentum of up to 15 GeV/c will interact with protons delivered by a cluster-jet target. Due to the  $4\pi$  detector surrounding the interaction point (IP), the cluster source and target beam dump each need to be located at a distance of 2.25 m and 2.35 m to the IP, respectively, connected by narrow jet beam pipes. For the success of this experiment, it is indispensable to achieve world record target thicknesses in such large distances to the nozzle and to develop a new state-of-the-art cluster-jet target.

A first prototype cluster-jet target was set up in Münster. Here, first investigations on beam properties were performed and crucial improvements were introduced [3,4]. Importantly, the maximal useful target thickness [5] of  $4.5 \cdot 10^{15}$  atoms/cm<sup>2</sup> at the IP was reached and even exceeded, here in a distance to the nozzle of 2.1 m, with a target thickness of  $(4.85 \pm 0.24) \cdot 10^{15}$  atoms/cm<sup>2</sup> [6].

Based on the obtained insights into the production of cluster-jets and setup handling, the final Münster Cluster-Jet Target was designed and built up, which is the topic of this article.

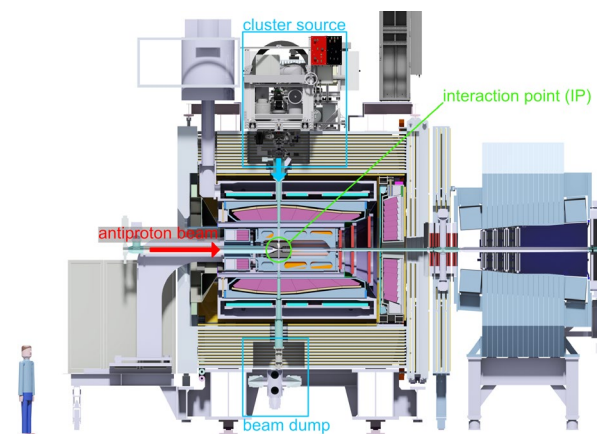


**Fig. 1.** Cross-section of the  $\bar{P}$ ANDA detector and the integrated  $\bar{P}$ ANDA cluster-jet target.

## 2 Münster Cluster-Jet Target for the $\bar{P}$ ANDA experiment

The cluster-jet target can be separated into several subcomponents (fig. 1): A cluster-jet source, which will be placed on top of the detector frame, will generate small droplets of hydrogen in the nm to  $\mu$ m scale, also referred to as clusters. These clusters will need to travel for 2.25 m as a cluster-jet through a narrow target vacuum beam pipe to the interaction point. There, they are going to interact with the antiprotons of the stored beam. Afterwards, all clusters that did not interact need to be dumped in the differentially pumped beam dump, which will be placed at a distance of 2.35 m to the interaction point.

The cluster-jet source and a first version of the beam dump are currently in operation at the Cooler Synchrotron COSY in Jülich, where first insights on the

\* Corresponding author: [s\\_vest01@uni-muenster.de](mailto:s_vest01@uni-muenster.de)

interaction of clusters with a stored proton beam were already obtained.

## 2.1 Cluster-Jet Source

Within the cluster-jet source (fig. 2), hydrogen is cooled down by a two-stage cold head to temperatures ranging from 20 to 40 K and pressed with typically 5 to 20 bar through a convergent-divergent Laval nozzle expanding into a first vacuum chamber. Due to vacuum conditions better than  $10^{-1}$  mbar, scattering with residual gas background is negligible. The resulting cluster-jet is separated from the gas background by a skimmer and afterwards tailored by a collimator, each optimizing the vacuum conditions of the differentially pumped stages. After a transition vacuum chamber, with a vacuum better than  $10^{-4}$  mbar, the cluster-jet is injected into the accelerator vacuum.

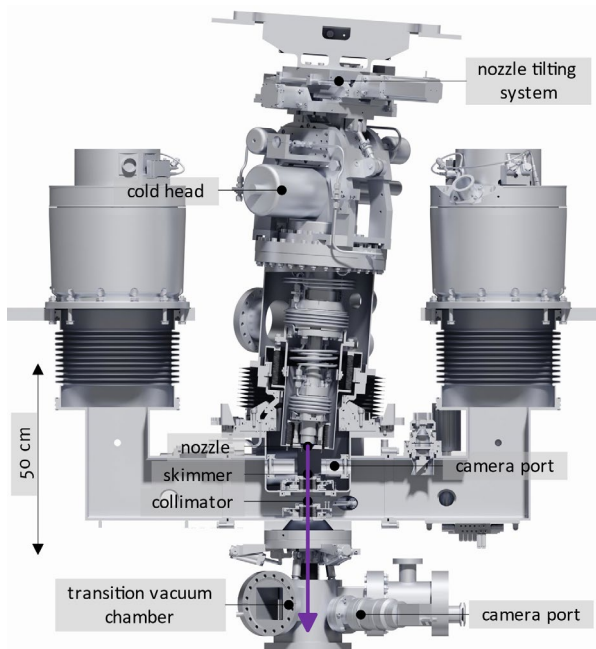


**Fig. 2.** Cluster-jet source. Cooled hydrogen is pressed through a Laval nozzle resulting in a defined cluster-jet propagating from top to bottom.

### 2.1.1 Convergent-divergent Laval Nozzle and Cluster Production Process

The convergent-divergent shape of Laval nozzles with narrowest diameters of approximately  $30\ \mu\text{m}$  leads to the possibility of forming hydrogen clusters, but is also a challenge in producing them.

Since the inner geometry needs to fulfil several special requirements, the desired Laval nozzles are not purchasable but need to be fabricated inhouse. Hence, a negative of the desired outlet is lathed out of aluminium. After a thin silver coating as separating layer, the negative is galvanized in a sulfuric acid copper bath by applying a DC current. As a sufficient diameter of copper is reached, the outer geometry is lathed and the convergent inlet is drilled. The most challenging part is now to drill the short connection channel between inlet and outlet of the nozzle as the resulting narrowest diameter is only  $30\ \mu\text{m}$ . Hence, this is a multi-step

drilling process. Afterwards the aluminium outlet negative is removed, and the final nozzle is obtained.

Within these nozzles, two different cluster production mechanisms are possible, depending on the state of the fluid upstream of the nozzle.

In general, the hydrogen is accelerated to the narrowest nozzle diameter due to the convergence of the nozzle inlet until it reaches speed of sound [7]. In the subsequent divergent outlet of the nozzle, assuming gaseous hydrogen, the atoms are further accelerated [8]. Due to adiabatic cooling, the relative momentum of the atoms is reduced leading to the formation of condensation nuclei by means of three-body interactions. Further impacts with the surrounding co-flowing cryogenic gas lead to a growth of the clusters until millions of atoms are accumulated in single clusters [7, 8]. Assuming, on the other hand, liquid hydrogen being in front of the nozzle, the atoms are also accelerated in the divergent outlet. Here, at appropriate operation conditions, i.e., for typical pressures between 5 and 20 bar and temperatures  $\geq 20\ \text{K}$ , the liquid hydrogen atomizes and forms a spray [9].

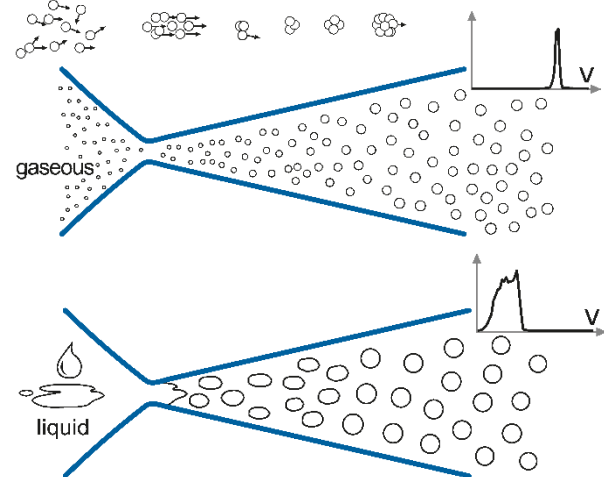


**Fig. 3.** Cluster production processes. *Top:* Clusters are formed from gaseous hydrogen by three-body interactions. *Bottom:* Clusters are formed from liquid hydrogen by an atomization process. Clusters formed from liquid hydrogen are larger and slower than clusters formed from gaseous hydrogen. (picture taken from [10])

Furthermore, when operating the cluster-jet target with liquid hydrogen, depending on the operational conditions, the resulting cluster-jet beam exposes high intense regions, referred to as core beams. Extracting these core beams allows for the desired high target thicknesses [6,11] of routinely  $10^{15}$  atoms/cm<sup>2</sup>. With different operation conditions smaller thicknesses are accessible. With gaseous hydrogen being in front of the nozzle, even thicknesses down to  $10^{13}$  atoms/cm<sup>2</sup> or less are possible.

### 2.1.2 Movable Skimmer and Collimator and Nozzle Tilting System

In order to separate the most intense core beam of the produced cluster-jet from its surrounding residual gas jet, a conical orifice, called skimmer, with an opening diameter of  $0.7\ \text{mm}$  allows for the jet to enter the next

vacuum chamber. A second conical orifice, called collimator, with an opening of  $800 \times 220 \mu\text{m}^2$  tailors the cluster-jet to its final rectangular shape further reducing the residual gas background.

After passing a transition vacuum chamber, the cluster-jet enters the target beam pipe. Over a distance of nearly 2 m, the pipe diameter is gradually reduced to 2 cm at the interaction point. In total, the most intense core beam of the cluster-jet needs to be aligned through nearly 5 m of the beam pipe to enter the beam dump and to reach highest target thicknesses at the interaction point. This can be achieved by tilting the nozzle and moving both the skimmer and collimator, which are each mounted on a stepper motor driven cross table.

## 2.2 Cluster-Jet Beam Dump

After passing the interaction point with the circulating antiproton beam, the remaining cluster-jet needs to be pumped away in a beam dump. Based on a prototype beam dump currently in operation, the final beam dump was developed. This beam dump will be located 2.35 m below the interaction point and will consist of three differentially pumped beam dump stages, which will be separated by adjustable orifices allowing to minimize the gas backflow (fig. 4). Additionally, within the beam dump several diagnostic tools will be implemented. These tools already have been tested and are described in the following.

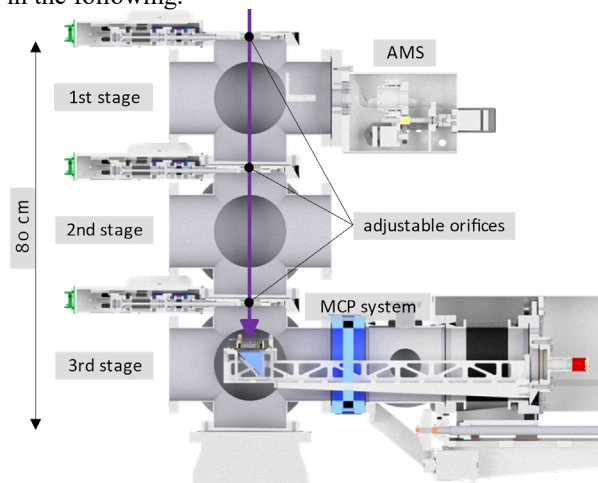


**Fig. 4.** Cluster-jet beam dump. After crossing the antiproton beam the cluster-jet will be dumped in the differentially pumped beam dump allowing for minimal gas backflow. Several beam diagnostic tools will be implemented.

### 2.2.1 Absolute Thickness Monitor System (AMS)

Within one of the beam dump stages, an absolute thickness monitor system will be installed. Here, two orthogonally oriented rods are moved one after another stepwise through the cluster-jet. Impinging clusters lead to a pressure increase proportional to the density of the cluster-jet. The pressure is measured depending on the rod position, which is shown in fig. 5. With the amplitude of the pressure profile normalized to the overlap of the moving rod and the cluster-jet  $p_{0/A}$ , the pumping speed  $S$ , the Avogadro constant  $N_A$ , the mean cluster velocity  $v$ , the universal gas constant  $R$  and the

ambient temperature  $T$ , the density  $\rho$  of the cluster-jet is determinable by

$$\rho_H = 2 \cdot \frac{p_{0/A} S N_A}{v R T} \quad (1)$$

and with this and the dimension of the cluster-jet also its thickness.

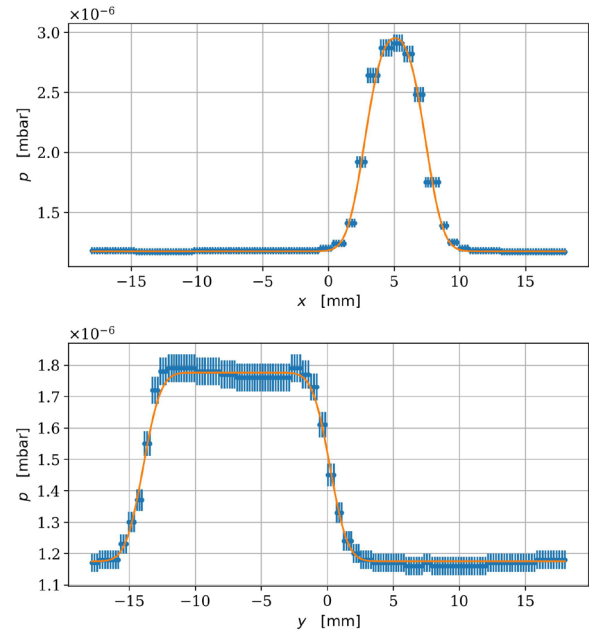


**Fig. 5.** Typical pressure profiles measured with the AMS in x- (top) and y-direction (bottom). From these profiles, the cluster-jet width in both directions and the actual position are directly observable. With further calculations (see eq. 1) also the cluster-jet density and the thickness are obtainable. It is to note that due to the rectangular collimator, also the cluster-jet has a rectangular cross-section with the long axis in particle beam direction (here y-direction) to maximize their overlap.

### 2.2.2 Multi-Channel Plate (MCP) System

Within the lowermost beam dump stage, an MCP system will be able to be moved into the cluster-jet allowing for several diagnostic analyses. It consists of a two-staged MCP in chevron assembly, a phosphor screen and a camera [12]. While taking data during the beam-target interaction at  $\bar{P}$ ANDA, the MCP system can be moved out of the cluster-jet, allowing for optimal vacuum conditions. Due to the small kinetic energy of neutral clusters and thus the negligible detection efficiency of the MCP, this system can only detect ionized clusters, which are accessible in two different ways.

In beam-target interactions during  $\bar{P}$ ANDA data taking operation, the antiproton beam only ionizes clusters in the vertex zone. These clusters hit the MCP and the subsequent electron avalanche lets the phosphor screen light up, which is detectable by the camera. Thus, an online vertex zone visualization with its two-dimensional size distribution is possible [12]. Moreover, with several calibration measurements it is possible to monitor the luminosity online during the  $\bar{P}$ ANDA experimental runs.

In combination with an electron gun, the total cluster-jet is ionized and thus visualized onto the phosphor screen. This is a useful tool in aligning the cluster-jet through its narrow beam pipe and is, after

calibration measurements with the AMS, a faster way of determining the cluster-jet thickness [13].

Furthermore, the electron gun can be operated in a pulsed mode. Within the time window for ionization of 20  $\mu\text{s}$ , a single cluster is ionized and thus the start signal for time-of-flight measurements is known. As this cluster hits the MCP system, the electron avalanche forms a voltage pulse at the phosphor screen, which can be measured and used as stop signal [13]. The time difference can then be used for a precise velocity measurement of single clusters leading to the cluster velocity distribution. From this, the mean velocity can be determined [7], which is needed for the thickness determination with the AMS as well as with the MCP system.

### 3 Summary

With the  $\bar{\text{P}}\text{ANDA}$  cluster-jet target, a state-of-the-art cluster-jet target will be available for a broad variety of experiments at the future HESR. In order to reach the desired high target thickness, liquified, pressurized hydrogen is fed through a specially designed and manufactured Laval nozzle. This results in a high-intense cluster-jet, which is extracted and shaped by a movable skimmer and collimator. The cluster-jet is guided over nearly 5 m through a target beam pipe, which has a width of down to 2 cm at the interaction point, until it is dumped in a differentially pumped beam dump. At the interaction point in 2.25 m distance to the nozzle, a target beam with a maximum thickness of up to  $4.5 \cdot 10^{15}$  atoms/cm<sup>2</sup> is placed in a high vacuum, with adjustable thickness over several orders of magnitude. Within the beam dump numerous self-developed diagnostic tools allow for determination of many properties as, e.g., cluster-jet position, cluster velocity, target thickness, target density, beam-target-interaction region, and luminosity. The delivered target is windowless and without any time structures. Furthermore, the target material is modifiable over a wide range of elements and compounds.

We want to acknowledge the support of the electrical and mechanical workshops in our institute for contributing to the final setup and the many steps in-between. This work was supported by BMBF, GSI F&E and HORIZON2020.

### References

1.  $\bar{\text{P}}\text{ANDA}$  Collaboration et al., *Strong Interaction Studies with Antiprotons*, arXiv: 0903.3905 (2009).
2. G. Barucca et al., *Eur. J. Phys A* **57**, 44, DOI: 10.1140/epja/s10050-021-00475-y (2021).
3. A. Täschner, Doctoral Thesis, Westfälische Wilhelms-Universität Münster (2012).
4. E. Köhler, Doctoral Thesis, Westfälische Wilhelms-Universität Münster (2015).
5.  $\bar{\text{P}}\text{ANDA}$  Collaboration, *Technical Design Report for the  $\bar{\text{P}}\text{ANDA}$  Internal Targets: The Cluster-Jet Target and Developments for the Pellet Target*. Technical report. FAIR. [panda.gsi.de/system/files/user\\_uploads/u.kurilla/R-E-TDR-2012-002.pdf](https://panda.gsi.de/system/files/user_uploads/u.kurilla/R-E-TDR-2012-002.pdf) (2012).
6. S. Grieser, Doctoral Thesis, Westfälische Wilhelms-Universität Münster (2018).
7. A. Täschner, E. Köhler, H.-W. Ortjohann, A. Khoukaz, *J. Chem. Phys.* **139**, DOI: 10.1063/1.4848720 (2013).
8. H. Pauly, *Atom, Molecule, and Cluster Beams 1*, Springer (2000).
9. C.C. Miesse, *Ind. Eng. Chem.* **47** (9), 1690–1701, DOI: 10.1021/ie50549a013 (1955).
10. S. Vestrick et al., *J. Supercrit. Fluids* **188**, DOI: 10.1016/j.supflu.2022.105686 (2022).
11. B. Hetz, Masters Thesis, Westfälische Wilhelms-Universität Münster (2017).
12. A. Khoukaz et al., *Nucl. Instrum. Methods Phys. Res. A* **735**, 12, DOI: 10.1016/j.nima.2013.08.085 (2014).
13. S. Vestrick, Masters Thesis, Westfälische Wilhelms-Universität Münster (2020).